

Magnetic study of spin freezing in the spin glass $\text{BaCo}_6\text{Ti}_6\text{O}_{19}$: Static and dynamic analysis

A. Labarta and X. Batlle

Departament de Física Fonamental, Universitat de Barcelona, Avenida Diagonal 647, 08028 Barcelona, Spain

B. Martínez and X. Obradors

Institut de Ciència de Materials de Barcelona, C.S.I.C., Campus Universitat Autònoma de Barcelona, 08193 Bellaterra, Spain

(Received 13 April 1992)

ac and dc magnetic susceptibility as a function of frequency, magnetic field, and temperature have been studied in polycrystalline $\text{BaCo}_6\text{Ti}_6\text{O}_{19}$. This oxide displays all the common features of spin-glass-like behavior. dc magnetic susceptibility at low fields shows a sharp peak at ca. 13.6 K, which signals the onset of irreversibility between the zero-field-cooled and field-cooled (FC) processes. Isothermal magnetization curves obtained from FC data have been fitted in terms of odd powers of $(\chi_0 H)$. The first two coefficients of the nonlinear susceptibility increase by more than three orders of magnitude when approaching T_c from above, thus indicating the occurrence of an equilibrium phase transition. Static scaling analysis of the nonlinear susceptibility leads to the following set of critical parameters: $\delta = 7.9 \pm 0.3$, $\phi = 5.7 \pm 0.5$, $T_c = 13.21 \pm 0.05$. The reliability of this set has been checked by reference to the asymptotic behavior of the scaling function. The unusually high values of the δ and ϕ exponents could be related to some degree of reduction of the spin dimensionality, because of the planar contribution to the anisotropy of Co^{2+} ions when located at octahedral sites. Dynamic scaling has been developed from ac susceptibility data assuming power-law divergence of the relaxation time, yielding the following set of parameters ($z\nu = 8.0 \pm 0.5$, $\beta = 0.75 \pm 0.10$, $T_c = 13.20 \pm 0.05$). The value of $z\nu$ has also been confirmed by studying the dependence of the freezing temperature on frequency. The β , δ , ϕ values roughly accomplish the scaling relation $\beta = \phi/\delta$. Thermoremanent-magnetization data show the common aging phenomena in disordered magnetic systems, as expected in spin glasses.

I. INTRODUCTION

In the last ten years, progress has been made in theoretical and numerical simulation work^{1,2} aimed at elucidating whether a spin-glass system undergoes a true equilibrium phase transition, although one question still remains unanswered: do experimental systems behave as theoretical models propose, and if so, does a true equilibrium phase transition occur?, or, on the contrary, can the spin-glass syndrome be explained only as a consequence of progressive freezing induced by magnetic frustration? As a consequence, there is still a general need to test critical theories in experimental systems with spin-glass-like behavior. In the context of this issue, we present a complete characterization of the critical behavior of a new insulating magnetic system with the typical spin-glass features.

Concerning three-dimensional (3D) Heisenberg spin-glass systems, a great number of experimental results are compatible with a phase transition at a finite temperature, characterized by a set of critical exponents³ that, in spite of their variations from one compound to another, may be considered as universal, taking into account experimental errors. Nevertheless, some controversy still surrounds lower spin and lattice dimensionality. For example, Gunnarsson *et al.*⁴ report a different set of critical exponents in a frustrated magnetic system with uniaxial anisotropy. In this framework, we show that these differences are also observed in other magnetic frustrated

systems with some degree of reduction of the spin dimensionality, such as on the $\text{BaCo}_6\text{Ti}_6\text{O}_{19}$ oxide.

$\text{BaCo}_6\text{Ti}_6\text{O}_{19}$ may be regarded as the compound obtained by total substitution of Fe ions by Co+Ti ions in the precursor *M*-type barium ferrite $\text{BaFe}_{12}\text{O}_{19}$. In the former oxide, the magnetic frustration leading to the spin-glass-like behavior arises from the cationic distribution of the doping cations among the five metallic crystallographic sublattices of the *M*-type structure. Nonmagnetic Ti^{4+} cations break the superexchange paths between magnetic Co^{2+} cations, making the collinear uniaxial magnetic structure of the pure phase unstable.

Previous neutron-powder-diffraction experiments⁵ showed that the cationic distribution is the following: $2a$ (83% Ti and 17% Co); $4e$ (20% Ti and 80% Co); $4f_{\text{IV}}$ (0% Ti and 100% Co); $4f_{\text{VI}}$ (83% Ti and 17% Co); $12k$ (55% Ti and 45% Co), where $2a$, $4f_{\text{VI}}$, and $12k$ are octahedral sublattices, $4f_{\text{IV}}$ is a tetrahedral sublattice, and $4e$ is a pseudotetrahedral site. The planar anisotropy of Co^{2+} cations when located in octahedral sites⁶ suggests a degree of reduction of the spin dimensionality, due to the considerable amount of Co^{2+} in this coordination, in our compound. We should remark that, although the pure precursor phase is always the same, other doping schemes of the *M*-type ferrites give rise to very different magnetic behavior, as a consequence of the hierarchy of preferences and the nature of the doping cations among the metallic sublattices. For example, in $\text{SrCr}_8\text{Ga}_4\text{O}_{19}$ the magnetic Cr^{3+} enters only in octahedral sites, leading

to a highly frustrated antiferromagnetic system with a set of coupled Kagomé-type magnetic lattices.⁷

The organization of this paper is as follows: After a brief introduction of experimental techniques, we present the results of the dc susceptibility experiments, from which the nonlinear part of the susceptibility is obtained and analyzed in the context of critical theories. In the third part, dynamic scaling analysis of the ac susceptibility in the range 5–1000 Hz, is performed. The value found for the $z\nu$ exponent is compared with that deduced from the dependence of the freezing temperature on the measuring frequency. Finally, thermoremanent magnetization is studied as a function of time, showing the characteristic aging phenomena previously observed in other spin-glass systems. Results are compared with other spin-glass systems.

II. EXPERIMENTAL

Polycrystalline $\text{BaCo}_6\text{Ti}_6\text{O}_{19}$ was synthesized by high-temperature solid-state reactions of stoichiometric BaCO_3 , TiO_2 , and Co_3O_4 mixtures. A detailed explanation of the thermal procedure is given in Ref. 5. The phase unicity of the final sample was verified from both x-ray and neutron diffraction. All reflections were indexed on the basis of the magnetoplumbite-type structure (structural group $P6/mmc$) and no extra peak was observed with respect to the precursor phase $\text{BaFe}_{12-2x}\text{Co}_x\text{Ti}_x\text{O}_{19}$.⁵

ac susceptibility measurements as a function of both frequency ($5 < \omega < 1000$ Hz) and temperature ($4.2 < T < 300$ K) were recorded with an ac Lake-Shore susceptometer in zero dc magnetic field and an ac magnetic field of 5 Oe. dc magnetic susceptibility and remanent magnetization measurements were carried out using a commercial superconducting quantum interference device (SQUID) magnetometer equipped with second-order gradiometer pickup coils in applied magnetic fields ranging from 1 to 50 kOe and temperatures between 4.2 K and room temperature.

The real and imaginary parts of the ac susceptibility were used to analyze the dynamic critical behavior.⁸ dc susceptibility was measured following both the zero-field-cooled (ZFC) and field-cooled (FC) processes, and the data obtained from the latter procedure were used to perform the static critical analysis. The time dependence of the thermoremanent magnetization was recorded after a FC process. A more detailed description of the relaxation measuring method is given in Ref. 9.

III. RESULTS AND DISCUSSION

A. dc susceptibility

In Fig. 1 we show the reciprocal low-field susceptibility (ca. 1 Oe) from 4.2 K up to room temperature. In the high-temperature regime ($T > 100$ K) the magnetic susceptibility displays typical Curie-Weiss behavior, from which a paramagnetic moment of $4.67\mu_B$ and a Curie temperature $\Theta = -80$ K are obtained. The value of the magnetic moment is within the theoretical $3.87\mu_B$ spin-only high-spin value of Co^{2+} ions when located in tetrahedral sites ($\langle L \rangle = 0$) and the $5.2\mu_B$ value usually

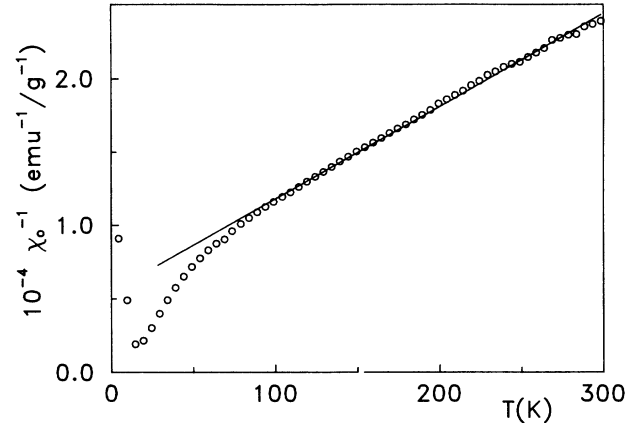


FIG. 1. Reciprocal low-field susceptibility (ca. 1 Oe) as a function of the temperature. The solid line represents high-temperature asymptotic Curie-Weiss behavior.

observed when located in octahedral sites ($\langle L \rangle \neq 0$).¹⁰ The negative sign of the Curie temperature suggests that the dominant interactions between the Co^{2+} magnetic moments are antiferromagnetic. Furthermore, a marked deviation from the linearity occurs below ca. 100 K, thus signaling the appearance of magnetic correlations among the Co^{2+} magnetic moments. This deviation increases with decreasing temperature, and a sharp peak appears at ca. 13.65 ± 0.05 K, which is associated with freezing phenomena of the Co^{2+} magnetic moments. Below this temperature, the magnetic irreversibility starts and the behavior of the sample depends on its magnetic history, leading to the differences observed in ZFC and FC susceptibility shown in Fig. 2. These features are the typical fingerprints of the spin-glass syndrome.

On the other hand, it is well known that the precursor compound, the pure M -type barium ferrite $\text{BaFe}_{12}\text{O}_{19}$, is ferromagnetic and the magnetic structure is uniaxial collinear to the c axis of the crystallographic structure.¹¹ Although the collinear structure is stable, all the dominant magnetic interactions are antiferromagnetic in such

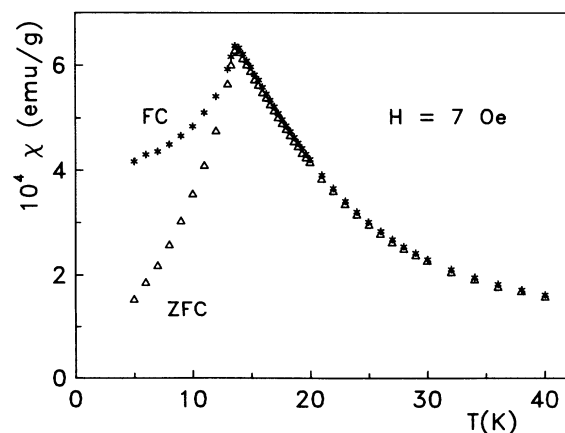


FIG. 2. Temperature dependence of the magnetization following a ZFC-FC process with a magnetic field of 7 Oe.

a way that none of them can be fulfilled simultaneously.¹² Thus, the cationic substitution rapidly alters the critical equilibrium of the superexchange paths that make the magnetic structure stable, which explains the appearance of new noncollinear magnetic structures in doped ferrites.¹³ In our case, the origin of the frustration in the $\text{BaCo}_6\text{Ti}_6\text{O}_{19}$ compound may be related to the random distribution of paramagnetic Co^{2+} ions and diamagnetic Ti^{4+} ions among the five metallic sublattices of the M -type crystallographic structure,⁵ inhibiting the appearance of long-range magnetic correlations. The topological frustration of the magnetic structure is measured by the ratio Θ/T_f , which in our compound is 6.1, being a typical value in spin-glass systems.¹⁴

To determine the nature of the freezing phenomenon that takes place at about 13.65 K we have studied the dependence of the FC magnetic susceptibility $\chi (=M/H)$ as a function of both temperature and applied magnetic field from which we derive the static critical behavior. In Fig. 3, χ is plotted against temperature between 10 and 30 K, with the applied magnetic field spanning from 10 to 40 kOe. From this figure we observe that the peak associated with the freezing phenomena broadens and becomes rounded as the field increases, due to the nonlinear effects.

However, the nonlinear contributions to the susceptibility are much more evident in Fig. 4, where susceptibility data at selected temperatures are represented as a function of the applied magnetic field. It is evident from this figure that the nonlinear contribution to the susceptibility increases substantially as the freezing temperature is approached from above. Therefore, the nonlinear contributions close to T_f are substantial even for fields as low as a few oersteds and so their effects must be taken into account in order to determine the correct linear susceptibility, as has been previously reported in other spin-glass systems.^{15,16} It is worth pointing out that the total sus-

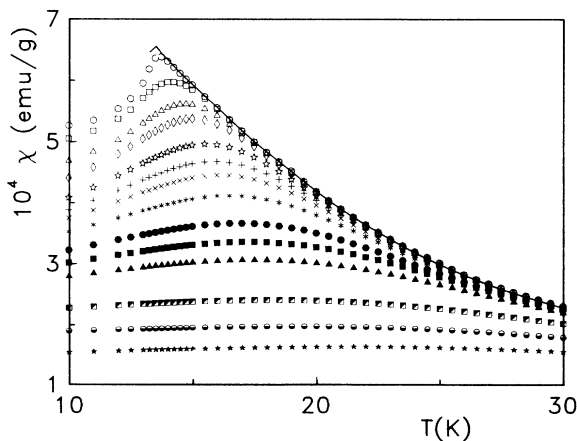


FIG. 3. Field-cooled magnetic susceptibility corresponding to different applied magnetic fields. The solid line corresponds to the χ_0 susceptibility obtained by fitting FC data to Eq. (1). Symbols are as follows: (\circ , 10 Oe), (\square , 120 Oe), (\triangle , 300 Oe), (\diamond , 500 Oe), (\star , 1 kOe), ($+$, 1.5 kOe), (\times , 2 kOe), ($*$, 3 kOe), (\bullet , 5 kOe), (\blacksquare , 7.5 kOe), (\blacktriangle , 10 kOe), (\blacksquare , 20 kOe), (\circ , 30 kOe), (\star , 40 kOe).

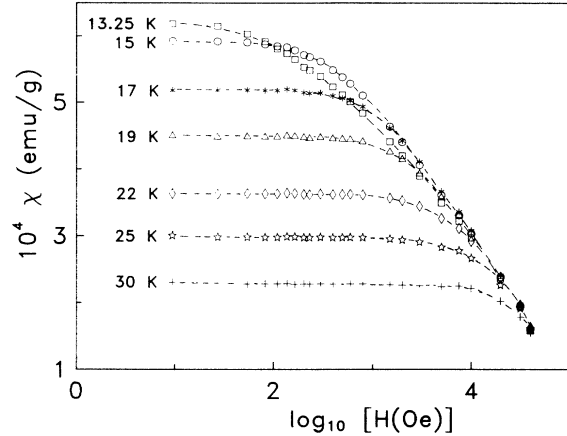


FIG. 4. Magnetic susceptibility at selected temperatures as a function of the logarithm of magnetic field.

ceptibility is temperature independent for fields higher than ca. 40 kOe signaling the saturation of the nonlinear part of the susceptibility.

B. Nonlinear analysis and power-law fits

In order to determine whether or not a canonical spin-glass transition takes place at T_f , we have analyzed the nonlinear contribution to the magnetic susceptibility by using the well-known development of the magnetization above T_f in terms of the odd powers of the field,¹⁷ which can be written in the following form:

$$M = \chi_0 H - b_3 (\chi_0 H)^3 + b_5 (\chi_0 H)^5 - \dots, \quad (1)$$

where the χ_0 coefficient is the linear susceptibility and the remaining coefficients stand for the nonlinear part. The least-squares fit of the isothermal magnetization curves obtained from the FC data to Eq. (1), shown in Fig. 3, allows the determination of the temperature dependence of the χ_0 , b_3 , and b_5 coefficients. Nevertheless, higher-order terms have been used in order to improve the fitting of the experimental data for temperatures close to T_f ; only the error bars of the first three coefficients were small enough to be used to study its temperature dependence. The temperature variation of these coefficients is shown in Fig. 5. Both b_3 and b_5 coefficients show a very strong upturn as T_f is approached from above, increasing their values by more than three orders of magnitude. This is often taken as proof of the existence of a true spin-glass transition.¹⁷ The behavior of the reciprocal linear susceptibility is also shown in the inset of Fig. 5. Curie-Weiss behavior is observed above $T = 18$ K, with a Curie temperature of $\Theta = 8 \pm 1$ K and a paramagnetic moment of $\mu = 2.7 \pm 0.2 \mu_B$, which is smaller than the value observed in the high-temperature paramagnetic regime. This indicates that an uncorrelated structure of frozen ferrimagnetic clusters takes place in the temperature range immediately above T_f . The value obtained for the Curie temperature indicates remaining ferromagnetic interactions among the frozen ferrimagnetic clusters.

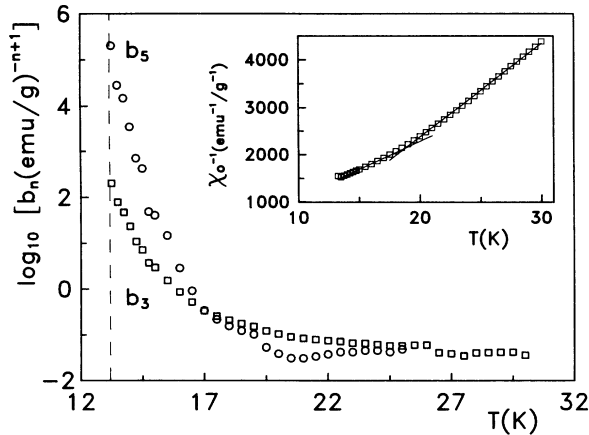


FIG. 5. Plot of the logarithm of the two first coefficients, b_3 and b_5 , of the expansion of the magnetization in odd powers of $(\chi_0 H)$ as a function of temperature. The reciprocal of the susceptibility at zero field, χ_0 , is shown in the inset. Straight lines show the regions in which effective Curie-Weiss law are obeyed.

C. Scaling analysis of the nonlinear susceptibility

The most relevant test of the critical behavior of a spin-glass system is obtained by measuring and analyzing the nonlinear part of the magnetic susceptibility defined by the equation

$$\chi_{nl}(H, T) = \chi_0(T) - M(H, T)/H, \quad (2)$$

where χ_0 is the linear susceptibility obtained by fitting experimental data to Eq. (1) (see Fig. 3). It is expected that χ_{nl} scales following the single-parameter relation¹⁸

$$\chi_{nl}(H, T) \propto H^{2/\delta} f(\epsilon/H^{2/\phi}), \quad (3)$$

where $\epsilon = (T - T_c)/T_c$, δ and ϕ are the critical exponents that rule the spin-glass transition, T_c is the critical temperature that signals the phase transition, and $f(x)$ is an arbitrary scaling function with the following asymptotic behavior

$$\begin{aligned} f(x) &= \text{const}, & x \rightarrow 0 \\ f(x) &= x^{-\gamma}, & x \rightarrow \infty. \end{aligned} \quad (4)$$

The exponent δ can be determined by the following equation:

$$\chi_{nl}(H, T_c) \propto H^{2/\delta}, \quad (5)$$

which represents the asymptotic behavior of the critical isotherm for x tending to 0. In the inset of Fig. 6 we show the log-log plot of χ_{nl} as a function of H . A δ value of 7.8 ± 0.3 is obtained from the slope of the linear regime. Using this value of δ the best data collapsing were obtained by varying the values of T_c and ϕ in Eq. (3). In Fig. 6 we show the best scaling of the experimental data $\chi_{nl}(H, T)$, which has been obtained with the following set of critical exponents: $\delta = 7.9 \pm 0.3$, $\phi = 5.7 \pm 0.5$, and $T_c = 13.21 \pm 0.05$. Only data above T_c with applied fields higher than 2 kOe have been used in this analysis.

The reliability of the set of critical exponents reported

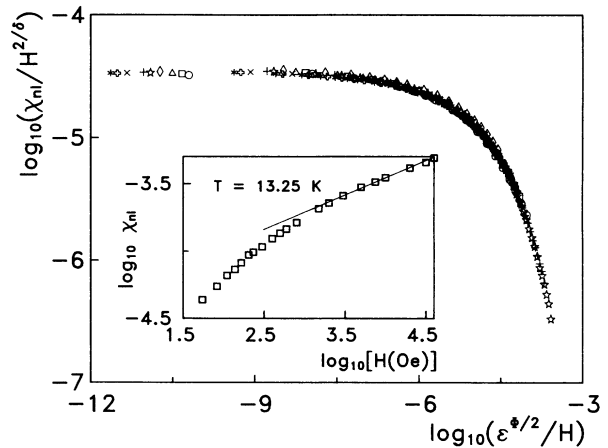


FIG. 6. Scaling plot of the nonlinear part of the susceptibility, χ_{nl} . Symbols correspond to the following values of the magnetic field: (\circ , 1.5 kOe), (\square , 2 kOe), (\triangle , 3 kOe), (\diamond , 5 kOe), (\star , 7.5 kOe), ($+$, 10 kOe), (\times , 20 kOe), (\diamond , 30 kOe), (\ast , 40 kOe). The inset shows the log-log plot of the χ_{nl} data, corresponding to the temperature 13.25 K, as a function of the magnetic field. The straight line stands for the asymptotic behavior.

before can be checked by studying the asymptotic behavior of the scaling function in the limits of $x \rightarrow 0$ and $x \rightarrow \infty$. In the limit of large x with constant magnetic field (i.e., at small fields or for large values of the reduced temperature, ϵ), an asymptotic behavior of the form $x^{-\gamma}$ is expected, γ being the susceptibility exponent related to δ and ϕ exponents through the scaling relation $\gamma = \phi(1 - 1/\delta)$. From the data in Fig. 6 we obtain an asymptotic slope of $-2\gamma/\phi = -1.6 \pm 0.2$, from which a value of $\gamma = 4.6 \pm 0.4$ is obtained, which is consistent with that obtained from the above scaling relation ($\gamma = 4.9 \pm 0.4$). On the other hand, in the $x \rightarrow 0$ limit, the constant behavior is observed as predicted from the asymptotic behavior of the scaling function.

The set of critical exponents we have obtained are significantly higher than those reported for other experimental spin-glass systems, especially those of the insulating type, for which typical values are $\delta = 4 \pm 0.5$ and $\phi = 3.5 \pm 0.5$.^{19,20} Nevertheless, some numerical results for the three-dimensional infinite-range Ising model suggest $\delta = 7.4$ and $\phi = 3.7$.¹ A recent paper by Gunnarsson *et al.*⁴ also reports a high value for the δ exponent ($\delta = 8.4 \pm 1.5$) in the short-range Ising spin-glass system $\text{Fe}_{0.5}\text{Mn}_{0.5}\text{TiO}_3$, in better agreement with our results. It should be noted that our results are also similar to those proposed for the crossover behavior corresponding to a 3D-2D system.²¹

D. Dynamic and analysis of the ac susceptibility

The study of the dynamical critical properties of this spin-glass system is very appealing from two points of view: on one hand, there is still a general need to test dynamical theories in spin glasses, and, on the other hand, it is also interesting to determine whether unusual values of the δ and ϕ exponents are confirmed with this analysis.

In-phase ac magnetic susceptibility shows a peak at low magnetic fields (see Fig. 7), which defines the spin-glass temperature, $T_f(\omega)$, which is not necessarily the phase transition temperature T_c . This temperature strongly depends on frequency of measurement (almost 1.5 K from 10 Hz to 1 kHz). However, the relative variation of T_f per frequency decade $\Delta T_f / (T_f \Delta \ln \omega)$ is 2.5×10^{-2} , which is intermediate between those typically reported for metallic spin glasses (0.7×10^{-2}) (Ref. 22) and for the insulator $\text{Eu}_{0.6}\text{Sr}_{0.4}\text{S}$ (5×10^{-2}).²³ This variation is very similar to that observed in the semimagnetic semiconductor system $\text{Cd}_{1-x}\text{Mn}_x\text{Te}$ (in particular for $x=0.4$).²⁴

By taking the temperature corresponding to the cusp of the in-phase ac susceptibility, $T_f(\omega)$, as the onset of strong irreversibility for each measuring time $t=1/\omega$ (ω is the frequency of the ac magnetic field) and studying its variation with the measuring frequency, it is possible to check the validity of the usual critical slowing down associated with a true phase transition for this system. If we assume an equilibrium phase transition, the divergence of the relaxation time τ as the critical temperature is approached from above is given by²⁵

$$\tau \propto [T_f(\omega)/T_c - 1]^{-z\nu}, \quad (6)$$

where ν is the critical exponent for the correlation length ξ , z is the dynamic exponent relating ξ and τ , and T_c is the phase transition temperature which has been set to the value obtained in the critical scaling of the nonlinear susceptibility. So, if the measuring frequency as a function of the reduced freezing temperature ($T_f/T_c - 1$) is represented in a log-log plot, the points are expected to be aligned over a straight line whose slope is the $z\nu$ exponent. This kind of plot for our data, giving a $z\nu$ value of 8.7, is shown in the inset of Fig. 8.

The definition of $T_f(\omega)$ used above is not accurate since it does not define a correct (H, T) line for a specific

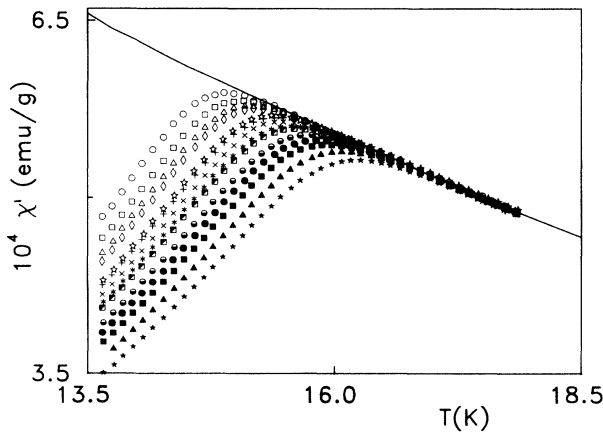


FIG. 7. In-phase ac susceptibility as a function of the temperature. The solid line represents equilibrium susceptibility obtained by fitting the FC data to Eq. (1). Symbols are as follows: (\circ , 8 Hz), (\square , 16 Hz), (\triangle , 25 Hz), (\diamond , 33 Hz), (\star , 57 Hz), ($+$, 74 Hz), (\times , 90 Hz), ($*$, 111 Hz), (\blacksquare , 153 Hz), (\ominus , 222 Hz), (\bullet , 333 Hz), (\blacksquare , 400 Hz), (\blacktriangle , 667 Hz), (\blackstar , 1000 Hz).

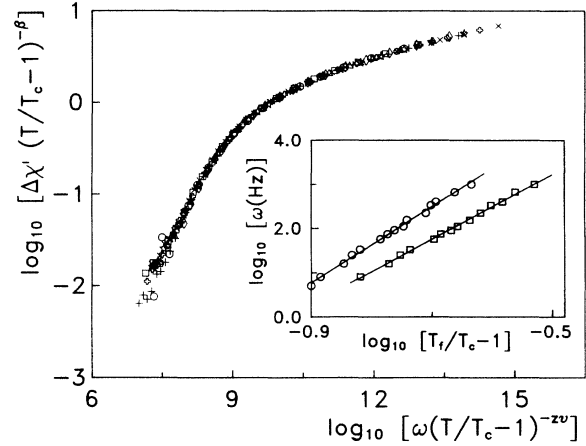


FIG. 8. Power-law scaling of $\Delta\chi'(T, \omega)$ data according to Eq. (8). Symbols are as follows: (\circ , 8 Hz), (\square , 16 Hz), (\triangle , 33 Hz), (\diamond , 74 Hz), (\star , 153 Hz), ($+$, 333 Hz), ($+$, 667 Hz), (\times , 1000 Hz). In the inset is represented the measuring frequency, ω , as a function of the reduced freezing temperature, $T_f/T_c - 1$, in a log-log plot. Open circles represent the freezing temperature determined as the cusp of the in-phase ac susceptibility, while squares correspond to the freezing temperature determined as that at which $|\chi''|/\chi'$ rise a constant arbitrary value.

response time τ , as has previously been pointed out by Bontemps *et al.*²⁶ It is clear that at a given measuring frequency ω , irreversible effects will appear at a temperature $T_i(\omega)$, defined by the onset of the out-of-phase susceptibility χ'' , which is higher than $T_f(\omega)$. It has previously been shown²⁶ that the critical dynamics of the system are better described by $T_i(\omega)$. Following the criterion proposed by Bontemps *et al.*²⁶ $T_i(\omega)$ may be defined at a constant response time τ for each observation time t ($t=1/\omega$), as the temperature at which $|\chi''|/\chi'$ is equal to a small arbitrary constant. In our case this constant value has been chosen to be 10^{-2} (this value must be greater than the noise-signal ratio). The dependence on the measuring frequency of the $T_i(\omega)$ obtained in this way is shown in the inset of Fig. 8. From these data we have obtained a value of the $z\nu$ exponent equal to 7.4, which is slightly smaller than that obtained from $T_f(\omega)$. The same disagreement between the results of these two methods of finding $z\nu$ has been previously observed in other spin-glass systems,²⁴ and it may be a consequence of the fact that $T_f(\omega)$ does not define a correct (H, T) line.

We have also studied the dynamic scaling of the quantity

$$\Delta\chi' = [\chi_{\text{eq}}(T) - \chi'(T, \omega)]\chi'_{\text{eq}}(T), \quad (7)$$

where the equilibrium susceptibility at zero frequency and zero magnetic field, $\chi_{\text{eq}}(T)$, has been assumed to be equal to the linear susceptibility, $\chi_0(T)$, deduced from the power-law fits of the isothermal magnetization curves to Eq. (1). In Fig. 7, the experimental $\chi'(T, \omega)$ data and the linear susceptibility $\chi_0(T)$ are simultaneously represented. It is clear from this plot that as the temperature in-

creases, the asymptotic behavior of the $\chi'(T, \omega)$ data perfectly matches the $\chi_0(T)$ curve (solid line), confirming the validity of our assumption. In the scaling region, where $\omega \rightarrow 0$ and $T \rightarrow T_c$, the quantity $\Delta\chi'$ can be written in the following form:

$$\Delta\chi' = \epsilon^\beta G(\omega \epsilon^{-z\nu}), \quad (8)$$

where β is the exponent of the order parameter, $G(x)$ the scaling function, and ϵ the reduced temperature defined before. In Fig. 8 we show the result obtained using the dynamic scaling law (8) for the full data $\Delta\chi'(T, \omega)$ at different frequencies and temperatures. The best data collapsing correspond to the set of values $z\nu = 8.0 \pm 0.5$, $\beta = 0.75 \pm 0.10$, and $T_c = 13.20 \pm 0.05$, which are in very good agreement, respectively, with the $z\nu$ value deduced from the study of $T_f(\omega)$ and $T_i(\omega)$, the critical temperature found in the static critical analysis, and even with the value of β predicted from the scaling relation $\beta = \phi/\delta = 0.72$ (using the values of ϕ and δ reduced from the static analysis). In fact, these values of the dynamic exponents compare well with those previously published for some semimagnetic semiconductor system²⁷ and also with results of numerical simulation corresponding to the case of three-dimensional spin glasses with short-range interactions.²⁸ We should remark that in a previous work⁸ we had carried out the dynamic scaling analysis for $\text{BaCo}_6\text{Ti}_6\text{O}_{19}$ using $\chi''(T, \omega)$ data, obtaining a very similar set of values for the critical exponents ($z\nu, \beta$) and for T_c .

In the preceding analysis, it is assumed that a true phase transition occurs at a finite temperature T_c . However, other models have been proposed that justify the appearance of a cusp in the $\chi'(T)$ curve. In the activated dynamic model²⁹ the system is considered as a set of superparamagnetic clusters, in which each cluster has a given probability of overcoming the anisotropy energy barrier. Associated with this energy barrier there is a relaxation time which is governed by either the Arrhenius or the Vogel-Fulcher laws.³⁰ In Ref. 8 we had tried to perform the scaling analysis of $\chi''(T, \omega)$ using this model but the degree of data collapsing obtained in this way was clearly worse. Furthermore, the values of the exponents obtained with the cluster model did not agree with any of the sets of exponents previously reported (for example, in semimagnetic semiconductors³¹). On the other hand, it has been reported that a fingerprint of activated dynamic behavior is an unusually large value of the $z\nu$ exponent (14 or larger) when data are analyzed in the scope of the power-law scaling.³¹ This fact is not observed in our compound, reinforcing the true phase assumption.

E. Thermoremanent magnetization as a function of time. Aging phenomena

Thermoremanent-magnetization data as a function of time were recorded after field cooling the sample from 50 K to a given temperature below T_f at which the sample was kept during the waiting time t_w , and the field was finally switched off before the measurements process started. The relaxation data were collected at 10 K (ca. $0.757T_c$), which is close enough to T_c to reveal aging phe-

nomena, the relaxation rate being slow enough to measure nonequilibrium magnetization even at very long times. The order of magnitude of the maximum value of the cooling magnetic field at which linear response is expected for this compound at temperatures close to T_c can be calculated from

$$\{\chi_0(T)/[b_3(T)\chi_0^3(T)]\}_{T \rightarrow T_c}^{1/2} = 10^3 - 10^2 \text{ Oe}. \quad (9)$$

The strength of the magnetic field used was 10 Oe, which seems to be small enough to ensure approximate linear response.

All the experimental $M_{\text{TR}}(t)$ curves (see Fig. 9) show an inflection point, when represented in a log-log plot, roughly located at the waiting time t_w , which is the time that the sample was kept at a constant temperature and field before the relaxation measurements started. This is the main consequence of the aging effects, since the system has not reached equilibrium when the field is switched off. So, as the observation time elapses, the system continues evolving as a function of the time $t_w + t_{\text{obs}}$.

Ocio, Alba, and Hammann have developed a phenomenological theory that allows quantitative estimation of the relaxation parameters. In this model, thermoremanent-magnetization data, $M_{\text{TR}}(T)$, are plotted as a function of an effective time defined by

$$\xi = \frac{t_0^{\mu-1}}{1-\mu} [(t+t_w)^{1-\mu} - t_w^{1-\mu}], \quad (10)$$

where the exponent μ must be fitted to satisfactorily superimpose the data in a unique master curve which represents the relaxation function of the system at a given constant age. The parameter t_0 is an arbitrarily chosen reference time ($t_0 = 1$ s) introduced to build ξ as a dimen-

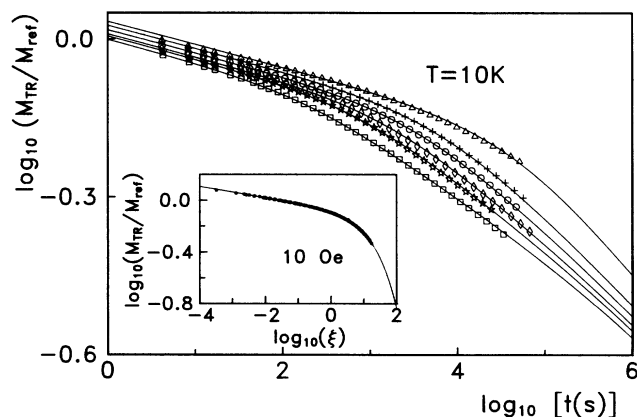


FIG. 9. Logarithm of the thermoremanent magnetization vs the logarithm of the observation time (in s) for different waiting times t_w at $T = 10$ K. The symbols correspond to the following values of the waiting time: (\square , 480 s), (\star , 1800 s), (\diamond , 3600 s), (\circ , 7200 s), ($+$, 14400 s), (\triangle , 90000 s). The solid lines are calculated from Eq. (11) using the values of the fitting parameters given in the text. The inset shows the master curve as a function of the reduced time, ξ . The solid line represents the fit of the experimental data to Eq. (11). M_{ref} is an arbitrary reference value.

sionless variable. The master curve obtained as a function of ξ can be fitted using the empirical law.

$$M_{\text{TR}}(\xi) = M_0 \xi^{-\alpha} \exp[-(\xi/\tau_p)^{1-n}], \quad (11)$$

where the sketched exponential accounts for aging phenomena, while the decreasing power law is the equilibrium relaxation of the system.

In the inset of Fig. 9, the master curve as a function of the reduced time ξ is shown in a log-log plot. The value of μ that gives good superposition of the data, corresponding to different waiting times, is $\mu = 0.83 \pm 0.05$. The master curve has been fitted to the empirical equation (11) and gives the following set of values for the parameters that characterize relaxation: $\alpha = 0.043 \pm 0.005$, $\tau_p = 50 \pm 15$, $n = 0.33 \pm 0.05$. These values are in very good agreement with those found in other insulating spin-glass systems measured at a comparable effective temperature [for example, in CsNiFeF_6 (Ref. 32) or in the thioespinel $\text{CdIn}_{0.3}\text{Cr}_{1.7}\text{S}_4$ (Ref. 33)]. It is evident that those in close agreement cannot be taken as unambiguous proof of the existence of the spin-glass state, since aging phenomena seem to be a common feature in many other frustrated magnetic systems. However, a true spin-glass system must show this phenomenology among other features which are also expected, such as those we have reported in Sec. II A, II B, II C, and II D.

IV. CONCLUSIONS

We have studied the dynamic and static critical behavior, as well as the thermoremanence as a function of time, of the $\text{BaCo}_6\text{Ti}_6\text{O}_{19}$ oxide.

Both dynamic and static critical analyses lead us to conclude that our system undergoes a true equilibrium phase transition at a finite temperature $T_f = 13.20 \pm 0.05$ K. The b_3 and b_5 coefficients of the development of the magnetization in terms of odd powers of the field show a strong upturn as T_f is approached from above, increasing their values by more than three orders of magnitude. This is usually associated with the occurrence of a true spin-glass transition. Moreover, the values of the critical exponents deduced from both analyses are compatible with the expected scaling relation $\beta = \phi/\delta$, which reinforces the consistency of the reported set of critical exponents. The value of the β exponent obtained from the ac susceptibility scaling is 0.75 ± 0.10 , while that deduced using the ϕ and δ values obtained from the dc scaling analysis and the scaling relation mentioned before is 0.72,

showing good agreement between them. The validity of the set of critical exponents has also been checked by reference to the asymptotic regimes in the critical region and studying the dependence of the freezing temperature on frequency. We have obtained a close agreement between the values deduced from the full data analysis and those derived from the latter produces.

The dynamical critical exponents $z\nu$ and β are within the variation range of those reported in some different kinds of spin-glass systems (metallic, short-range, semimagnetic, uniaxial spin glasses, etc.) In any case, the β value 0.75 ± 0.1 is somehow smaller than the expected value in Heisenberg and Ising spin-glass cases (1.0 and 0.9, respectively). On the other hand, the $z\nu$ value 8.0 ± 0.5 is also in very good agreement with Monte Carlo simulation results²⁸ and renormalization-group calculations³⁴ in Ising spin-glass systems.

Concerning static scaling, our set of experimental critical exponents are significantly higher than those reported in the literature for the majority of 3D Heisenberg spin glasses ($\delta = 7.9 \pm 0.3$, $\phi = 5.7 \pm 0.5$). Nevertheless, large values of the δ exponent have been also reported from numerical simulation,¹ experimental critical analysis for a short-range Ising spin-glass system,⁴ and systems exhibiting a 3D-2D crossover behavior.²¹ In our present case, some degree of reduction of the spin dimensionality of the Co^{2+} might be induced by the planar anisotropy of these cations when located in octahedral sites. This fact might explain the unusually high values of the δ and ϕ critical exponents. Presently, we are trying to obtain high-quality $\text{BaCo}_6\text{Ti}_6\text{O}_{19}$ single crystals in order to perform critical analysis and so confirm the reduction of the spin dimensionality.

We also performed⁸ the activated scaling analysis of the ac data in order to verify the validity of the cluster model,²⁹ for which a true phase transition does not occur, but the degree of data collapsing in this way was clearly worse. Although the cluster model should not be completely ruled out as an explanation of the freezing phenomena in our sample, the self-consistency of the preceding analysis suggests that the spin-glass freezing is a more consistent explanation.

We would like to remark that the thermoremanent-magnetization data show the usual aging phenomena observed in many kinds of disordered system. This cannot be taken as proof of the existence of the spin-glass state, although a true spin-glass system must display all these features.

¹K. Binder and A. P. Young, *Rev. Mod. Phys.* **58**, 801 (1986).

²*Heidelberg Colloquium on Glassy Dynamics*, edited by J. L. Van Hemmen and I. Morgenstern, *Lecture Notes in Physics*, Vol. 275 (Springer-Verlag, Heidelberg, 1987).

³P. Beauvillain, C. Dupas, J. P. Renard, and P. Veillet, *Phys. Rev. B* **29**, 4086 (1984).

⁴K. Gunnarsson, P. Svedlindh, P. Nordblad, L. Lundgren, H. Aruga, and A. Ito, *Phys. Rev. B* **43**, 8199 (1991).

⁵X. Batlle *et al.* (unpublished).

⁶J. C. Slonczewski, *Phys. Rev.* **110**, 1341 (1958); D. J. De Bitet-

to, *J. Appl. Phys.* **35**, 3482 (1964); F. Bolzoni and L. Pareti, *J. Magn. Magn. Mater.* **42**, 44 (1984); A. Collomb, P. Wolfers, and X. Obradors, *ibid.* **62**, 57 (1986).

⁷X. Obradors *et al.*, *Solid State Commun.* **65**, 189 (1988); A. P. Ramírez, G. P. Espinosa, and A. S. Cooper, *Phys. Rev. Lett.* **64**, 2070 (1990).

⁸X. Batlle, A. Labarta, B. Martínez, X. Obradors, V. Cabañas, and M. Vallet-Regí, *J. Appl. Phys.* **70**, 6172 (1991).

⁹A. Labarta, R. Rodríguez, L. Balcells, J. Tejada, X. Obradors, and F. J. Berry, *Phys. Rev. B* **44**, 691 (1991).

- ¹⁰E. A. Boudreaux and L. N. Mulay, *Theory and Applications of Molecular Paramagnetism* (Wiley, New York, 1976).
- ¹¹E. W. Gorter, Proc. IEEE **104B**, 225 (1957); X. Obradors, A. Collomb, M. Pernet, D. Samaras, and J. C. Joubert, J. Solid State Chem. **56**, 171 (1985); A. Collomb, P. Wolfers, and X. Obradors, J. Magn. Magn. Mater. **44**, 57 (1986).
- ¹²A. Isalgué, A. Labarta, J. Tejada, and X. Obradors, Appl. Phys. **A39**, 221 (1986).
- ¹³G. Albanese, G. Asti, and P. Batti, Nuovo Cimento B **54**, 339 (1968); **58**, 467 (1968); X. Obradors, A. Collomb, M. Pernet, and J. C. Joubert, J. Magn. Magn. Mater. **44**, 118 (1984); X. Obradors, A. Isalgué, A. Collomb, A. Labarta, M. Pernet, J. A. Pereda, J. Tejada, and J. C. Joubert, J. Phys. C **19**, 6605 (1986).
- ¹⁴A. P. Ramírez, J. Appl. Phys. **70**, 5952 (1991).
- ¹⁵A. P. Malozemof, Y. Imry, and B. Barbara, J. Appl. Phys. **53**, 7672 (1982).
- ¹⁶F. Bensamka, D. Bertrand, A. R. Fert, and J. P. Redoules, J. Phys. C **19**, 4741 (1986).
- ¹⁷R. Omari, J. J. Prejean, and J. Souletie, J. Phys. (Paris) **44**, 1069 (1983).
- ¹⁸J. Chalupa, Solid State Commun. **22**, 315 (1977); M. Suzuki, Prog. Theor. Phys. **58**, 1151 (1977).
- ¹⁹H. Maletta and W. Felsch, Phys. Rev. B **20**, 1245 (1979).
- ²⁰E. Vincent and J. Hammann, J. Phys. C **20**, 2659 (1987).
- ²¹A. Gavrin, J. R. Childress, C. L. Chien, B. Martínez, and M. B. Salamon, Phys. Rev. Lett. **64**, 2438 (1990).
- ²²J. L. Tholence, Physica B+C **126B**, 157 (1984).
- ²³J. Ferré, J. Rajchenbach, and H. Maletta, J. Appl. Phys. **52**, 1697 (1981).
- ²⁴A. Mauger, J. Ferré, M. Ayadi, and P. Nordblad, Phys. Rev. B **37**, 9022 (1988).
- ²⁵P. C. Hohenberg and B. I. Halperin, Rev. Mod. Phys. **49**, 435 (1977).
- ²⁶N. Bontemps, J. Rajchenbach, R. V. Chamberlin, and R. Orbach, Phys. Rev. B **30**, 6514 (1984).
- ²⁷Y. Zhou, C. Rigaux, A. Mycielsky, M. Menant, and N. Bontemps, Phys. Rev. B **40**, 8111 (1989).
- ²⁸A. T. Ogielsky, Phys. Rev. B **32**, 7384 (1985).
- ²⁹J. Villain, J. Phys. (Paris) **46**, 1843 (1985); D. S. Fisher, Phys. Rev. Lett. **56**, 416 (1986).
- ³⁰J. L. Tholence, Solid State Commun. **35**, 113 (1980).
- ³¹S. Geschwind, A. T. Ogielsky, G. Devlin, J. Hegarty, and P. Bridenbaugh, J. Appl. Phys. **63**, 3291 (1988).
- ³²M. Ocio, M. Alba, and J. Hammann, J. Phys. (Paris) Lett. **46**, L1101 (1985).
- ³³M. Alba, J. Hammann, M. Ocio, P. Refregier, and H. Bouchiat, J. Appl. Phys. **61**, 3683 (1987).
- ³⁴D. S. Fisher, J. Appl. Phys. **61**, 3672 (1987).